Theory of *T* junctions and symmetric tilt grain boundaries in pure and mixed polymer systems

Daniel Duque, K. Katsov, and M. Schick
Department of Physics, University of Washington, Seattle, Washington, 98195-1560

(Received 29 July 2002; accepted 16 September 2002)

We apply self-consistent-field theory to *T* junctions and symmetric tilt grain boundaries in block copolymer systems with and without the addition of homopolymer. We find that, in the absence of homopolymer, *T* junctions have a larger free energy per unit area than that of the symmetric tilt junctions with which they compete except for a range of angles between about 100° and 130°. With the addition of homopolymer, this range increases. These results are quite consistent with experiment. As the angle between grains increases towards 180°, the *T* junction undergoes a morphological change somewhat similar to that which occurs in symmetric tilt grain boundaries. At the onset of this change, the free energy per unit area decreases markedly. © *2002 American Institute of Physics.* [DOI: 10.1063/1.1519537]

I. INTRODUCTION

Modulated phases appear in diverse systems, from semiconductor inversion layers,[1] to neutron stars.[2] The most common phases exhibiting modulation are lamellar, hexagonal, and several cubic ones.[3] It is rare that a system can be prepared in a pure grain of such a phase. More commonly the system is rife with defects such as grain boundaries at which grains of different orientation meet. Such defects are important because they affect the material properties of the system, and as such have been well studied, particularly in crystalline solids.[4] However there are advantages in studying grain boundaries in smectics, such as the lamellar phases formed by block copolymers, due to the fact that there is no order parallel to the lamellae themselves. As a consequence, only three angles are required to specify a grain boundary as opposed to the five which are required in crystalline solids.[5]

Defects in block copolymer systems have received much experimental attention.[6–10] The challenging problem of the calculation of their properties, particularly the free energy per unit area of grain boundaries, has received less scrutiny.[11–14] For the system of block copolymers, however, considerable progress can be made as self-consistent-field theory (SCFT) provides a powerful tool to investigate the phases of these systems, including the modulated ones.[15] The application of SCFT to grain boundaries in block copolymer systems was pioneered by Matsen,[13] who considered symmetric tilt boundaries in lamellar phases. It was later applied to twist grain boundaries of these phases by Duque and Schick.[14]

A symmetric tilt boundary, or kink grain boundary (KGB), can be thought of as being produced by bending a uniform lamellar phase such that the normals to the lamellae far from the boundary make an angle θ with one another (see Fig. 1). The lamellae are not twisted with respect to one another, a condition which fixes the value of the second angle. The grain boundary is located along the plane of symmetry, which fixes the third angle, one we denote by ψ, to be zero. We show in Fig. 1 that in a symmetric tilt grain boundary of angle $180° - \theta$, the lamellae far from the grain boundary have the same orientation as those for a boundary of angle θ. One sees, however, that their energies must be very different; thus there is no symmetry about an angle of 90°.

A third configuration in which the lamellae have the same orientation far from the boundary is the *T* junction, shown in Fig. 1(d). Here the grain boundary runs along the lamellae of one of the grains. With ψ measuring the angle between the grain boundary and the bisector of the two normals, the *T* junction is specified by $\psi = (180° - \theta)/2$. The energy per unit area of the *T* junction is easily seen to be symmetric about $\theta = 90°$.

If the directions of the lamellae within the grains are fixed during the nucleation of the phase, one might expect the frequency of occurrence of these configurations to be proportional to Boltzmann factors involving their energies. Burgaz and Gido[10] noted that the occurrence of *T* junctions was greatly enhanced in a mixture of copolymer and homopolymer over that in a pure copolymer system in which they rarely occurred. They argued that the presence of homopolymer relieved stress near the tips of those lamellae which end abruptly in the *T* junction, lowering the energy of this configuration. Their experimental results and strong-segregation theory calculations indicated that, if the blocks are labeled *A* and *B* and the homopolymer consists of *A*, then the lamellae which end abruptly are those consisting of the minority *B* component.

In this paper we employ SCFT to calculate the free energy per unit area of these different grain boundaries in both pure diblock, and mixed diblock, homopolymer systems. We find in the pure diblock system that the free energy per unit area of the *T* junction is higher than that of the symmetric KGB except for a range between about 100° and 130°. The addition of homopolymer comparable to that used in experiment causes this range to increase, encompassing angles between about 85° and 140°. We confirm that the lamellae which end abruptly at a *T* junction are those of the minority component.

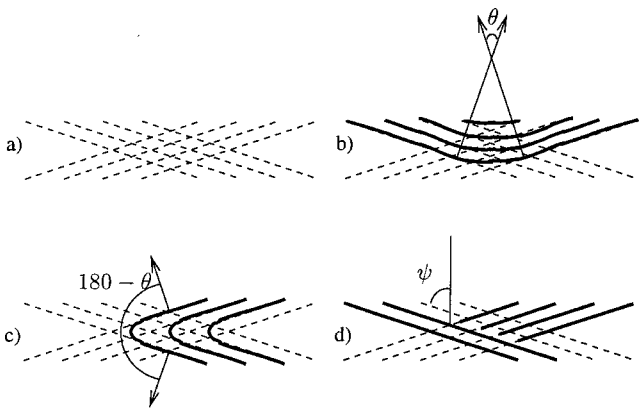

FIG. 1. Some possibilities for a particular set of grains: (a) phantom grains, to show the geometry, (b) a KGB of angle θ, (c) a KGB of angle $180° - \theta$, and (d) a T junction.

Of particular interest is the change in morphology of the T junctions as the angle θ approaches 180°. We find that the lamellae which will end abruptly at the boundary change their direction near it so that they effectively run parallel to the lamellae in the other grain. This is reminiscent of the change from chevron to omega morphology in the symmetric tilt boundary.[8,12,13]

In the next section, we summarize the theoretical framework of SCFT, and the approach we take to solve the equations. In Sec. III we present our results, first for normal incidence, $\theta = 90°$, and then for other angles. We conclude with a discussion.

II. THEORY

We apply SCFT to a T junction of angle θ. One half of the system is shown in Fig. 2 because we have taken the full system to be symmetric about the x axis. We have included in the full system only one and one half wavelengths of the grain whose lamellae run parallel to the x axis, a simplification which is justified as we find negligible distortion produced in the lamellae near $y=0$ by the presence of the lamellae of the other grain. The system is periodic in the x direction, with wavelength $D/\sin\theta$, where D is the bulk lamellar wavelength. Note that this assumed periodicity precludes the occurrence of any increase in the lamellar spacing in the region of the end caps.[10]

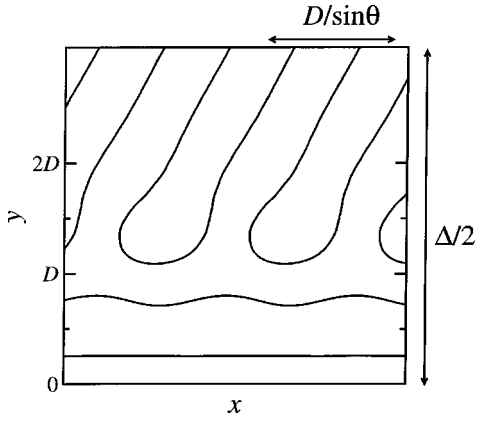

FIG. 2. Illustration of the system considered.

Our approach is basically that of Ref. 13, so we need only to summarize it here. We consider a mixture of linear AB diblock copolymers and A homopolymers. The former occupy a volume fraction $1-\phi$, and are characterized by N statistical segments of which half make up the A block, and the other half the B block (i.e., $f=1/2$ in the usual notation). This choice is motivated by the system used in the experiment of Ref. 10. The copolymer considered there is actually a three-arm A_2B copolymer with an f of 0.38, but as discussed[16] by the same authors, this corresponds to a linear AB copolymer with an $f \approx 1/2$. Although our copolymer is not a star, but linear, we expect that the crucial feature for the enhancement of T junctions reported in experiment is the addition of homopolymer, not the architecture of the copolymer.[17] The homopolymers occupy a volume fraction ϕ and are composed of αN statistical segments. We take $\alpha = 0.015$, again motivated by experiment,[10] and consider several volume fractions of homopolymer, $0<\phi<0.3$. We assume Gaussian segments with the same statistical length, and common volume $1/\rho_0$. Incompressibility is enforced, and the A, B repulsion is characterized by the Flory–Huggins parameter χ.

In the SCFT, the Helmholtz free energy is given by[18]

$$\frac{N}{V\rho_0 kT}F = (1-\phi)\log(1-\phi) + \frac{\phi}{\alpha}\log\phi + (1-\phi)\log Q_c + \frac{\phi}{\alpha}\log Q_h + \frac{\chi N}{V}\int d\mathbf{r}\,\phi_A(\mathbf{r})\phi_B(\mathbf{r}) - \frac{1}{V}\int d\mathbf{r}[w_A(\mathbf{r})\phi_A(\mathbf{r}) + w_B(\mathbf{r})\phi_B(\mathbf{r}) + \xi(\mathbf{r})(\phi_A(\mathbf{r})+\phi_B(\mathbf{r})-1)], \quad (1)$$

and is to be extremized with respect to the A and B monomer density distributions $\phi_A(\mathbf{r})$ and $\phi_B(\mathbf{r})$, and the three fields $w_A(\mathbf{r})$, $w_B(\mathbf{r})$, and $\xi(\mathbf{r})$. The minimization yields the self-consistent set of equations

$$\phi_A(\mathbf{r}) + \phi_B(\mathbf{r}) - 1 = 0, \quad (2)$$

$$\phi_A(\mathbf{r}) - \phi_B(\mathbf{r}) + (w_A(\mathbf{r}) - w_B(\mathbf{r}))/\chi N = 0, \quad (3)$$

$$(\phi_A(\mathbf{r}) + \phi_B(\mathbf{r}))/2 - (w_A(\mathbf{r}) + w_B(\mathbf{r}))/2\chi N + \xi(\mathbf{r}) = 0, \quad (4)$$

where the density distributions are given by

$$\phi_A(\mathbf{r}) = (1-\phi)\frac{\delta \log Q_c}{\delta w_A(\mathbf{r})} + \frac{\phi}{\alpha}\frac{\delta \log Q_h}{\delta w_A(\mathbf{r})}, \quad (5)$$

$$\phi_B(\mathbf{r}) = (1-\phi)\frac{\delta \log Q_c}{\delta w_B(\mathbf{r})}. \quad (6)$$

The partition function, Q_c, is that of a single copolymer in external fields w_A and w_B acting on A and B segments, respectively, while Q_h is that of a single homopolymer in an external field w_A. They can be expressed, as usual, in terms of Green's functions satisfying a modified diffusion equation.

Questions are sometimes raised[19,20] about the numerical details of the procedure employed to solve the SCFT equa-

tions. We have used both Broyden's method for systems of nonlinear equations and a simpler iterative technique of the type called "nonconserved relaxational dynamics" in Ref. 19. In the latter, an amount proportional to the left-hand side of Eq. (2) is added to the sum of the fields, and another proportional to the left-hand side of Eq. (3) is subtracted from the difference of the fields. Even though Broyden's method can be very fast in many instances, it can also be quite unstable or lead to unstable solutions, so in general we prefer the simpler method. For each one of these choices, one can choose to solve the diffusion equations either in real or Fourier space. The former is more flexible and intuitive, but here we use the Fourier technique,[15] which in this case requires a smaller computational cost to achieve a given accuracy. Finally, as an initial guess for the first iteration, we usually make an ansatz for the difference of density distributions, $\Delta\phi \equiv \phi_A - \phi_B$, from the known bulk lamellar result, $\Delta\phi_0$,

$$\Delta\phi = (1-f(y))\Delta\phi_0(ky) + f(y)\Delta\phi_0(k_x x + k_y y), \quad y \geqslant 0, \tag{7}$$

where $k = 2\pi/D$, $k_x = k\sin\theta$, $k_y = k\cos\theta$, and $f(y)$ is a simple Fermi–Dirac function going from $f(0) = 1/2$ to $f(\infty) = 1$. This we translate to the difference in the fields by Eq. (3). For the sum of the fields, which is not so obvious to guess, we simply set $\xi = 0$ everywhere and improve upon that.

The structure in Fig. 2 can be expanded with the following choice of Fourier basis functions:

$$f_{mn}(x,y) = \begin{cases} c_m c_n \cos(mk_x x)\cos(nk_\Delta y), & \text{even } n, \\ c_m c_n \cos(mk_x x)\cos(nk_\Delta y), & \text{odd } n, \end{cases} \tag{8}$$

where m, $n = 0,1,2,...$ and $k_\Delta = \pi/\Delta$. The normalization coefficients are $c_m = \sqrt{2}$, except for $c_0 = 1$. The system is taken to be periodic in the y direction with wavelength Δ. This choice is for computational convenience and should be of no consequence provided that Δ is sufficiently large. (We use $\Delta = 10\sqrt{6}R_g$ for the results that we present here, where R_g is the radius of gyration of the copolymer.) Our computational resources require truncation of the expansion at typical values of 8 for m and 60 for n. This is sufficient to yield free energies which are within 0.3% of the actual value and free energies per unit area within 1.5%, an error barely noticeable in the scale of our plots.

III. RESULTS

A. Normal incidence

In this case, $\theta = 90°$, calculation of the T junction is simpler, as the sine terms in Eq. (8) are absent. In Figs. 3 and 4 we present results for the surface free energy per unit area, γ, obtained, as in Ref. 13, from the excess free energy:

$$\frac{N\gamma}{\rho_0 kT\sqrt{6}R_g} = \left(\frac{N(F-F_b)}{V\rho_0 kT}\right)\left(\frac{\Delta/2}{\sqrt{6}R_g}\right), \tag{9}$$

where F_b is the free energy of the bulk system in the absence of the grain boundary.

We examine the dependence of γ on the segregation parameter χN for a pure copolymer ($\phi = 0$). We see in Fig. 3

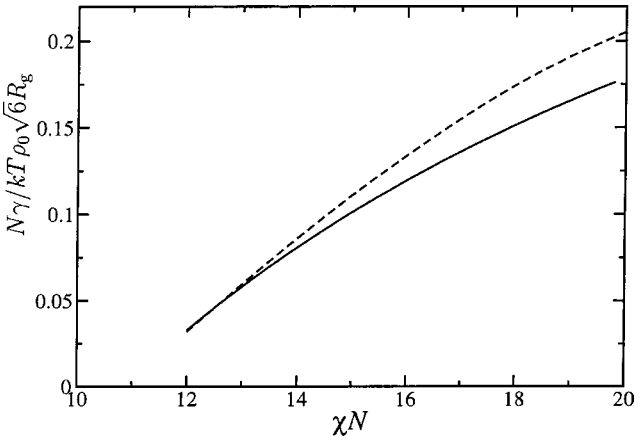

FIG. 3. Surface free energy per unit area as a function of segregation, χN, for a pure copolymer system; solid line, KGB; dashed line, T junction.

that, for strong enough segregation, the normal T junction always has a larger surface energy, γ_T, than the normal KGB, γ_K. For $\chi N < 13$, however, the two are almost equal, γ_T being actually lower for $\chi N < 12.4$. Note that the value for $\chi N = 20$ is very close to the prediction by Matsen[13] of 0.2, based upon previous work.[12,21]

In Fig. 4(a) we plot the location of the intermaterial dividing surface (IMDS) between A- and B-rich regions, defined by $\phi_A = \phi_B = 1/2$. One sees very little variation in the location of this surface with the exception of some modulation of the lamella and of the end caps. This kind of structure is very similar to that seen experimentally in the few pure copolymer T junctions reported in Ref. 8, and calculated previously utilizing Landau theories adequate in the weak segregation regime.[12,22]

Next, we fix $\chi N = 20$ and study the effect of adding A homopolymer of volume fraction ϕ. This addition breaks the symmetry between T junctions in which the capped lamellae are composed of A and those in which they are composed of

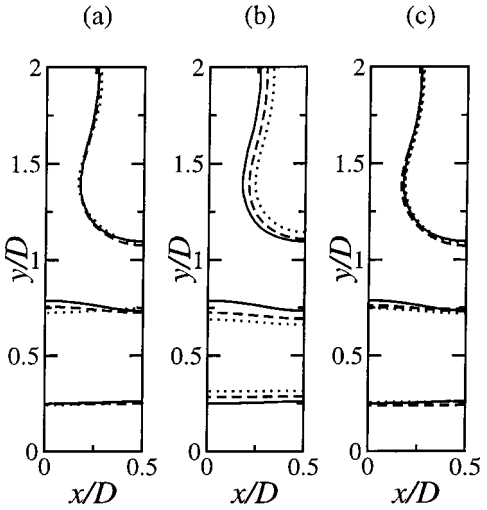

FIG. 4. IMDS for various systems: (a) pure copolymer system at different segregations χN: 20 (solid line), 16 (dashed line), and 12 (dotted line) (b) for the T junction (b) at $\chi N = 20$, for $\phi = 0$ (solid lines), $\phi = 0.2$ (dashed line) and 0.3 (dotted line), (c) same as in (b), but plotting the copolymer-only IMDS.

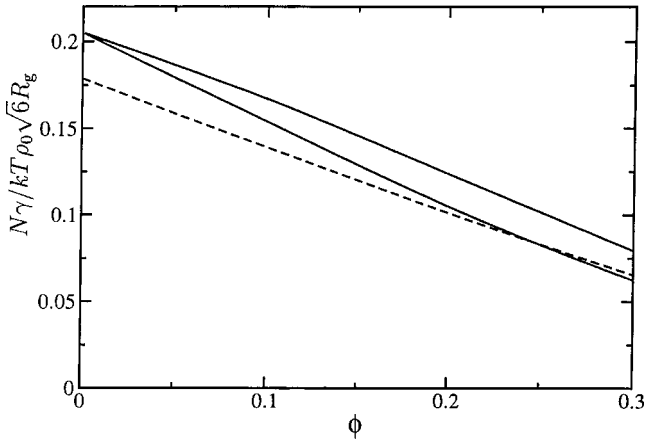

FIG. 5. Surface free energy per unit area at $\chi N=20$ as a function of homopolymer volume fraction ϕ, for the KGB (dashed line) the *T* junction (a) (upper solid line) and *T* junction (b) (lower solid line).

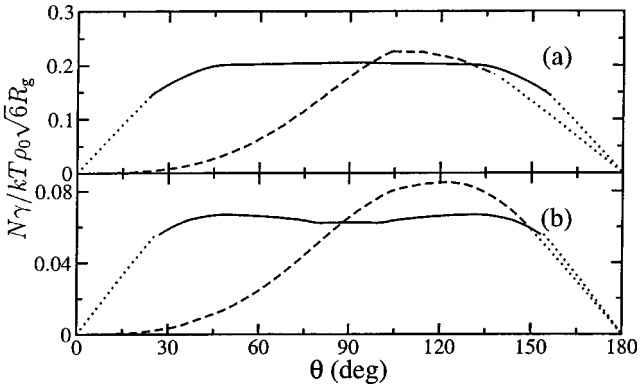

FIG. 6. Surface free energy per unit area as a function of tilt angle at $\chi N=20$ for the KGB (dashed line), and the *T* junction (solid line); (a) pure copolymer system, (b) homopolymer fraction of $\phi=0.3$. The dotted lines are fits based on the idea of isolated dislocations: $\lambda \sin\theta/D$ for the *T* junctions and $2\lambda\cos(\theta/2)/D$ for the KGB.

B. We denote the former as *T* junction (a), and the latter as *T* junction (b). They correspond to cases 2 and 4 in Ref. 10.

As Fig. 5 shows, *T* junction (b) always has a surface free energy which is lower than that of *T* junction (a), so the former is the morphology expected to be observed, as indeed it is in experiment. We expect the difference in surface free energies to be more pronounced in the experimental cases, since $\chi N>60$ there.[17] We also observe that *T* junction (b) becomes the configuration of lowest surface free energy when the *A* homopolymer fraction, ϕ, exceeds 0.25. In the experiment of Ref. 10, $\phi\approx 0.2$.

The IMDS for $\phi=0.2$ and $\phi=0.3$, again defined as the point at which $\phi_A=\phi_B=1/2$, is shown in Fig. 4(b). As expected, the addition of *A* homopolymer swells the *A* regions. We shown in Fig. 4(c) the points at which $\phi_B=(1-\phi)(1-f)$, i.e., those points at which the copolymer density attains its mean value, a kind of copolymer-only IMDS. This shows how the copolymer relaxes at the *AB* interfaces due to the partial relief of copolymer stretching that a short, solvent-like, homopolymer brings about, a phenomena discussed at length in Ref. 18. The effect is small, but can be seen by comparing Figs. 4(b) and 4(c). Whereas the former shows that the addition of *A* homopolymer causes the IMDS to move inward toward the *B*-rich regions of the lamellae as expected, the latter figure shows that this addition causes the copolymer-only IMDS at the tip of the end cap to move slightly in the opposite direction.

We have also examined the extent of any enhancement of homopolymer concentration close to the end caps, which would correspond to cases 3 and 5 in Ref. 10. To do so, we have shifted from the canonical ensemble of our calculations to the grand canonical ensemble, and fixed the bulk chemical potentials so that the densities are those of the bulk lamellar phase. The density profiles are indistinguishable in the scale of Fig. 4, so that any such enhancement effect is quite minor.

B. Non-normal incidence

We now present our results for *T* junctions for which the angle θ between grain normals differs from 90°. In Fig. 6(a) we show the surface free energy per unit area in the pure copolymer system for both the KGB and the *T* junction. The KGB free energy, as discussed in Refs. 12 and 13, vanishes as θ^3 for small angles. As this free energy is not convex, it signals that such small angle KGBs are unstable. For larger θ however, the symmetric tilt boundaries are stable, and their free energy reaches a maximum around 120°. It then decreases, probably linearly, as $\theta\rightarrow 180°$. There is a smooth change from chevron to symmetric omega structures[12,13] at about $\theta=90°$, and a symmetry-breaking transition to an asymmetric omega[13] at about $\theta=110°$. The free energy per unit area of the *T*-junction reaches a plateau extending over a wide range of angles about normal incidence. It is as if the end caps act as hinges, so that a change in tilt were without cost. It is not clear whether this surprising result, which does not contradict experiment, expresses some interesting physics, or is simply due to a fortuitous cancellation of different effects. Further study is needed to illuminate this point. The free energy then decays linearly to zero at smaller and greater angles. Note that the free energy of the *T* junction is lower than that of the symmetric tilt grain boundary for a range of angles extending from about 100° to 130°. They are sufficiently close to one another at 90° that it is not surprising both kinds of grains are observed in the same sample, as in Fig. 2(c) of Ref. 8.

In Fig. 6(b) we show the corresponding result for the system with added *A* homopolymer of volume fraction $\phi=0.3$. As the symmetry is already broken by the presence of homopolymer, there is no phase transition to the symmetry-broken omega KGB. The behavior of the free energy of the *T* junction is not greatly affected by the homopolymer, although its absolute value certainly is. There is again a plateau with a very shallow minimum for normal incidence, or very close to it. The numerical resolution we use does not permit us to determine the exact location of the minimum. We observe that the free energy per unit area of the *T* junction is now less than that of the KGB over a wider range of angles extending from a bit less than 90° to about 140°. Furthermore, the difference between the free energies of the two structures is greatest near 120°. As noted earlier, the *T* junction structure and free energy is symmetric about 90° so

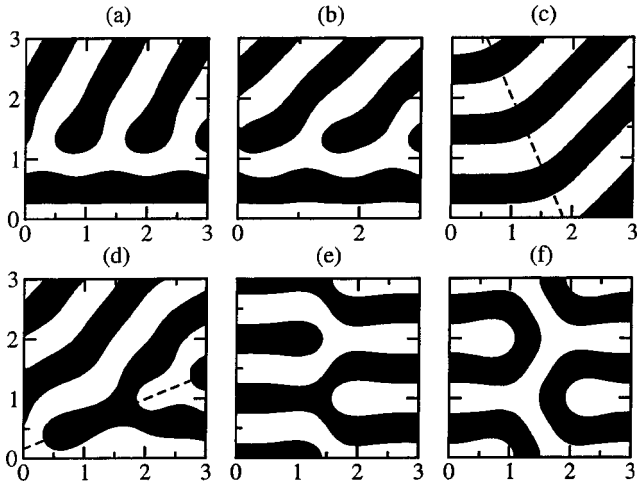

FIG. 7. Different structures; for clarity, one of the regions has been shown black, with the IMDS separating black and white regions. (a) $\theta=60°$ T junction, (b) $\theta=45°$ T junction showing the "sock" structure, (c) KGB at $\theta=45°$ (the dashed line is the grain boundary line), (d) KGB at $\theta=180°-45°$ (the dashed line is the grain boundary line), (e) structure to approximate the Y1 edge defect, (f) structure to approximate the Y2 edge defect. All results are for pure copolymer at $\chi N=20$, with lengths given in units of D.

that this maximum corresponds to a peak in the occurrence of T junctions which would be assigned to an angle of about 60°. Indeed there is a peak in the distribution of T junctions with angle around 50° as measured in Ref. 10.

We show in Figs. 7(a) and 7(b) results for the IMDS for the T junctions of $\theta=60°$ and 45°. These confirm the picture that can be extracted from the free energy itself: for angles close to the normal there is little deformation of the lamellae except for the presence of the end caps. As the angle θ decreases, these end caps begin to spread along the opposing lamellae, eventually forming a kind of "sock" structure. This is quite analogous to the transformation from chevron to omega which occurs in the tilt grain boundary.[13] Such "sock" structures can be clearly seen in Fig. 11 of Ref. 8 which shows a region of T junction.

IV. DISCUSSION

When discussing the experimental results for the symmetric tilt and T-junction structures, one must keep in mind the fact that they are metastable structures. Presumably they result from a complicated process that can be history dependent, so that a theoretical description should be dynamical, like that[23] based on the Swift–Hohenberg model.

Still, some important information can be extracted from our equilibrium results. For example, a general feature of several grain boundaries at very large angles is that they consist of defects which become progressively isolated as the angle θ is increased. Large angle tilt boundaries are composed of edge dislocations, while large angle twist grain boundaries are composed of screw dislocations.[11,14]

One can see from Fig. 7(b) that the $\theta=45°$ T junction resembles a series of edge dislocations separated by a spacing of $D/\sin\theta$. Each one of these dislocations consists of a Y-shaped region, shown in white, enveloping an end cap, shown in black. These defects become isolated in the limits $\theta\to 0°$ and $\theta\to 180°$. In principle, their line energy, λ, could be extracted because, in these limits, the free energy per unit area, γ, takes the limiting form $\gamma\to\lambda\sin\theta/D$. In practice, such a calculation is difficult because it requires a very large number of Fourier components. This reflects the fact that as $\theta\to 0°$ or 180°, the periodicity in the x direction increases without limit as does the distance in the y direction over which the perturbation, due to the grain boundary, relaxes. Nevertheless we are able to approach this limit sufficiently to justify fitting our results for γ to the limiting form given above. The best such fit is shown by dotted lines in Fig. 6, and from it we obtain $N\lambda/kT\rho_0(6R_g^2=0.55$ in the pure system, and 0.19 in the presence of homopolymer with volume fraction $\phi=0.3$. For comparison, we can calculate an approximate value for the line energy of this defect by means of the structure shown in Fig. 7(e). In it, we have Y defects on both sides. Defects of the same kind are separated by a distance D along the y axis so the line energy of each one would be

$$\frac{N\lambda}{kT\rho_0 6R_g^2}\approx\left\langle\frac{N(F-F_b)}{VkT\rho_0}\right\rangle\left\langle\frac{D\Delta/2}{6R_g^2}\right\rangle, \tag{10}$$

similar to Eq. (9). (Our system has, again, the size $\Delta/2$, this time along the x axis). This approximation ignores the attractive interaction between defects which are very close together, and thus must yield a line energy lower than the actual value of an isolated defect. Indeed the values for λ we obtain this way are, in the same units as above, 0.38 for the pure system, and 0.11 for the system with homopolymer. This approximate result can be improved in a systematic way by taking the defects to be further from one another, but the study of isolated defects necessitates greater computational power. We note that the grain boundary of Fig. 7(e) is analogous to an "antiphase boundary" [24] in antiferromagnets. Its free energy per unit area is $\gamma=0.232$ and 0.076 in the systems with $\phi=0$ and 0.3 volume fractions of homopolymer. The units of free energy per unit area are those of Eq. (9).

The situation is also quite interesting for the symmetric tilt grain boundary. We show in Figs. 7(c) and 7(d) the two structures which could compete with the T junction of $\theta=45°$; the symmetric tilt boundaries of $\theta=45°$ and $\theta=(180-45)°$. They separate the same grains, but the boundary between grains is a different one, and is shown with a dashed line. Figure 7(d) shows an angle-dependent behavior which had already been suggested by Matsen in Ref. 13. The symmetry-broken omega morphology, after departing from the symmetric chevron one at about $\theta=100°$, seems to return to a symmetric state for higher angles. Note in Fig. 7(d) that the white domains are starting to develop protrusions which are similar to the black ones. If such a symmetric state did occur for the tilt boundary then, as comparison of Figs. 7(b) and 7(d) shows, this grain boundary would consist of the same Y defects as occur in the T junction, and it is not difficult to show that their energies approach one another. We expect $\gamma\to 2\lambda\cos(\theta/2)/D$, a fit shown in Fig. 6. On the other hand, if the tilt boundary morphology remained symmetry broken even as $\theta\to 180°$, a circumstance which our calcula-

tions indicate is unlikely, then the grain boundary would consist of defects like those shown in Fig. 7(f). The line tensions in the same units as above are now $\lambda = 0.50$ and 0.17, for the cases $\phi = 0$ and $\phi = 0.3$, respectively. Note that this grain boundary separates two domains with the same orientation; the free energy per unit area is $\gamma = 0.302$ and 0.109.

These calculations are included to show how one might obtain the limiting behavior of the surface tension by an independent calculation of the line tension of the line defects.

In conclusion, we have calculated the free energies per unit area of *T* junctions in block copolymer systems with and without the addition of homopolymer and compared them to those of symmetric tilt grain boundaries with which they compete. We found that in the pure diblock system, the *T* junctions are favored over a range of angles between about 100° and 130°, but the free energy difference is small. The addition of homopolymer causes the *T* junctions to be favored for a larger range of angles, a range which grows with homopolymer volume fraction. Further, the relative difference between the two structures in free energy per unit area increases, which implies that the *T* junctions within this range become more stable. The free energy per unit area of the *T* junction is rather constant over a range of angles in which the morphology of the truncated lamellae is rather unaffected save for the appearance of endcaps. Their free energy decreases rather rapidly, however, beyond a certain angle at which their morphology changes significantly, with the terminating lamellae changing direction as they approach the grain boundary to parallel the boundary itself and the lamellae in the grain on the other side of it. As the angle between grains approaches 180°, the free energy of the symmetric tilt boundary becomes lower than that of the *T* junction, so that, in principle, the former will be favored. In practice we expect the two junctions to become indistinguishable at such large angles.

ACKNOWLEDGMENTS

The authors would like to thank David Andelman, John Cahn, Sam Gido, and Yoav Tsori for numerous invaluable exchanges. This work was supported in part by grants from the United States–Israel Binational Science Foundation under Grant No. 98-00429, and the National Science Foundation under Grants Nos. DMR 9876864 and DMR 0140500. D.D. acknowledges support from the Spanish Ministry of Education and Sport.

[1] A. Koulakov, M. Fogler, and B. Shklovskii, Phys. Rev. Lett. **76**, 499 (1996).
[2] C. Pethick and D. Ravenhall, Annu. Rev. Nucl. Part. Sci. **45**, 429 (1995).
[3] F. Bates and G. Fredrickson, Phys. Today **52**, 32 (1999).
[4] A. Sutton and R. Balluffi, *Interfaces in Crystalline Materials* (Clarendon, Oxford, 1995).
[5] J. Cahn (unpublished).
[6] S. Gido, J. Gunther, E. Thomas, and D. Hoffman, Macromolecules **26**, 4506 (1993).
[7] Y. Nishikawa, H. Kawada, H. Hasegawa, and T. Hashimoto, Acta Polym. **44**, 247 (1993).
[8] S. Gido and E. L. Thomas, Macromolecules **27**, 6137 (1994).
[9] T. Hashimoto, S. Koizumi, and H. Hasegawa, Macromolecules **27**, 1562 (1994).
[10] E. Burgaz and S. Gido, Macromolecules **33**, 8739 (2000).
[11] R. D. Kamien and T. C. Lubensky, Phys. Rev. Lett. **82**, 2892 (1999).
[12] R. Netz, D. Andelman, and M. Schick, Phys. Rev. Lett. **79**, 1058 (1997).
[13] M. Matsen, J. Chem. Phys. **107**, 8110 (1997).
[14] D. Duque and M. Schick, J. Chem. Phys. **113**, 5525 (2000).
[15] M. Matsen and M. Schick, Phys. Rev. Lett. **72**, 2660 (1994).
[16] D. Pochan, S. Gido, S. Pispas, and J. Mays, Macromolecules **29**, 5099 (1996).
[17] S. Gido (private communication).
[18] M. Matsen, Macromolecules **28**, 5765 (1995).
[19] G. H. Fredrickson, V. Ganesan, and F. Drolet, Macromolecules **35**, 16 (2002).
[20] F. Schmid, J. Phys.: Condens. Matter **10**, 8105 (1998).
[21] M. Matsen, J. Chem. Phys. **106**, 7781 (1997).
[22] Y. Tsori and D. Andelman, J. Chem. Phys. **115**, 1970 (2001).
[23] D. Boyer and J. Viñals, Phys. Rev. E **65**, 046119 (2002).
[24] J. Cahn and R. Kikuchi, J. Phys. Chem. Solids **20**, 94 (1961).